FULL PAPER

Magnetic Resonance in Medicine 00:00–00 (2016)

A Look-Locker Acquisition Scheme for Quantitative Myocardial Perfusion Imaging with FAIR Arterial Spin Labeling in Humans at 3 Tesla

Graeme A. Keith,[1]* Christopher T. Rodgers,[1] Michael A. Chappell,[2] and Matthew D. Robson [1]

Purpose: A novel method for quantitative measurement of myocardial blood flow (MBF) using arterial spin labeling (ASL) in a single breath-hold is presented, evaluated by simulations, phantom studies and in vivo studies and tested for reproducibility and variability.

Methods: A flow-sensitive alternating inversion recovery (FAIR) ASL method with Look-Locker readout (LL-FAIR-ASL) was implemented at 3 tesla. Scans were performed on 10 healthy volunteers and MBF measured in three slices. The method was investigated for reproducibility by Bland-Altman analysis and statistical measures, the coefficients of reproducibility (CR) and variation (CV) are reported.

Results: The MBF values for the basal, mid, and apical slices were 1.04 ± 0.40, 1.06 ± 0.46, and 1.06 ± 0.38 ml/g/min, respectively (mean $\pm$ SD), which compare well with literature values. The CV across all scans, 43%, was greater than the between-session and within-session values, at 16 and 13%, respectively, for the mid-ventricular slice. The change in MBF required for detection, from the CR, was 61% between-session and 53% within-session for the mid-ventricle.

Conclusion: This study shows the feasibility of the LL-FAIR-ASL method for the quantification of MBF. The statistical measures reported will allow the planning of future clinical research studies involving rest and stress measurements. **Magn Reson Med 000:000–000, 2016.** **© 2016 The Authors Magnetic Resonance in Medicine published by Wiley Periodicals, Inc. on behalf of International Society for Magnetic Resonance in Medicine. This is an open access article under the terms of the Creative Commons Attribution License, which permits use, distribution and reproduction in any medium, provided the original work is properly cited.**

Key words: ASL; MBF; FAIR; heart; human

INTRODUCTION

Cardiovascular magnetic resonance (CMR) imaging is a powerful tool for the investigation of common pathologies of the heart such as congenital heart disease, coronary artery disease, and cardiomyopathies (1). One of the most useful processes that CMR allows us to investigate is the perfusion of blood in the myocardial tissue. In clinical practice, this is achieved with the use of an intravenous extracellular contrast agent, such as Gadolinium-DPTA (2), where the transit of the agent through the capillary bed of the myocardium can be observed. These first-pass techniques provide clinically applicable methods of imaging perfusion, but suffer from several drawbacks, such as significant problems with image artifacts (3), cost, the risk of the contrast agent itself to patients with renal conditions (4), and the difficulty of performing multiple serial evaluations owing to the lingering presence of the contrast agent.

An attractive alternative to first-pass perfusion CMR techniques and other, nuclear based modalities, such as single-photon emission computed tomography (SPECT) (5,6) or positron emission tomography (PET) (7,8), would be to use arterial spin labeling (ASL). ASL is a noninvasive technique which uses magnetic labeling strategies to allow the proton spins present in the blood water to act as an endogenous contrast agent (9,10). In one of the simplest ASL experiments, known as flow-sensitive alternating inversion recovery (FAIR) (11,12), two images or sets of images are collected, one in which a globally selective (GS) inversion pulse is applied before the readout (the control image) such that the spins of the myocardial tissue of interest and those of the inflowing blood are both inverted. The second image set is preceded by a slice-selective (SS) inversion through a slice of the myocardium (the tag or label image) such that the myocardial tissue in the imaging slice is again inverted but the blood water spins flowing into the image slice remain in thermomagnetic equilibrium. The effect of the presence of these inflowing spins in the SS experiment is to cause an apparent shortening of the longitudinal relaxation time (T_1) of the tissue. It is the size of the difference in the observed T_1 values between the two measurements that allows us to quantitatively evaluate the blood flow to the myocardium.

The measurement of T_1 values in the myocardium, often in the form of T_1 mapping techniques, has emerged as a useful tool in CMR (13). One established, robust method often used for T_1 mapping is the modified Look-Locker inversion recovery (MOLLI) (14–16) sequence and it's variants, which allow for the measurement and parametric mapping of the myocardial T_1 in vivo, in a single breath-hold. In this approach, an inversion pulse is applied and the relaxation of the longitudinal magnetization is sampled following an inversion time, TI, then

[1]Oxford Centre for Clinical Magnetic Resonance Research, University of Oxford, John Radcliffe Hospital, Oxford, United Kingdom.

[2]Institute of Biomedical Engineering, University of Oxford, Old Road Campus, Oxford, United Kingdom.

Grant sponsor: MRC; Grant number: G0900883; Grant sponsor: the Wellcome Trust; Grant sponsor: the Royal Society; Grant number: 098436/Z/12/Z.

*Correspondence to: Graeme A. Keith, Oxford Centre for Clinical Magnetic Resonance Research, University of Oxford, John Radcliffe Hospital, Oxford, UK OX3 9DU. E-mail: graeme.keith@cardiov.ox.ac.uk

Received 4 May 2016; revised 28 July 2016; accepted 28 July 2016

DOI 10.1002/mrm.26388

Published online 00 Month 2016 in Wiley Online Library (wileyonlinelibrary.com).

© 2016 The Authors Magnetic Resonance in Medicine published by Wiley Periodicals, Inc. on behalf of International Society for Magnetic Resonance in Medicine.

again following the equivalent of one R–R interval, measured by electrocardiograph (ECG) -gating, and so on to build up a relaxation curve allowing the quantification of T_1. Different variants of the technique use different inversion-readout schemes (3(3)3(3)5 for MOLLI, 5(1)1(1)1 for ShMOLLI and so on, indicating the number of look-locker images acquired and the duration of the gaps between acquisitions, all in units of heart beats).

In this work, a method for measuring myocardial blood flow (MBF) noninvasively using a FAIR labeling scheme combined with a Look-Locker acquisition (LL-FAIR-ASL) (17) is presented. The described method allows for the acquisition of both FAIR inversion states (SS and GS) within a single breath-hold. The method is assessed by way of simulation, phantom study, and in vivo application. The method is further used for quantitative analysis of MBF in healthy volunteers. MBF is measured in three slices in humans with ASL for the first time and is assessed for reproducibility and variability.

METHODS

Sequence Design

The LL-FAIR-ASL sequence was implemented on a 3 tesla (3 T) whole-body scanner (TIM Trio, Siemens, Germany). The sequence consisted of two HS8 adiabatic inversion pulses (18), one SS, one GS with a duration of 10 ms, time/bandwidth product $R = 40$ and $\beta = 3.45$. Each inversion pulse was followed by a block of five cardiac triggered balanced steady-state free precession (bSSFP) readouts (19). The readout consisted of LISA excitation pulses, which are Gaussian-like, and included five initial ramp-up pulses and a final half-alpha "restore pulse." The two inversion blocks were separated by a gap of three heartbeats to allow for some recovery of the magnetization, within a manageable breath-hold, as shown in Figure 1, thus forming a MOLLI 5(3)5 regime. Both SS and GS inversions were collected in a single thirteen heartbeat breath-hold. The ordering scheme of the sequence within this thirteen heart beat breath-hold (SS-GS or GS-SS) was varied. Sequence parameters were based closely on those used successfully in MOLLI implementations and included a 35° excitation flip angle, image slice thickness of 8 mm, an initial TI of 115 ms (with the following values being 115 ms + RR, 115 ms + 2RR,...), TR/TE of 3 ms/1.5 ms, 320 mm field of view with 75% phase resolution and 6/8 partial Fourier, a 192×144 image matrix (interpolated to 384×288) and an acceleration factor of GRAPPA 2 (20). All inversion pulses and readouts occurred during the diastolic phase of the cardiac cycle. This timing guaranteed that the signal recovery was not corrupted by through-plane bulk cardiac motion, by restricting inversions and readouts to the most stable cardiac phase. Due to the inversion recovery nature of the sequence at least 15 s was allowed between scans to allow for full relaxation of the magnetization.

Simulation

Bloch simulations of the sequence were performed in MATLAB (The Mathworks Inc., Natick, MA) with the acquisition parameters defined above and not accounting for magnetization-transfer effects. The inversion pulses were simulated fully as HS8 pulses with the parameters matching those described above and the power set as per the scanner maximum output voltage to simulate the actual B_1 power used on the scanner to ensure the adiabatic condition is met. The evolution of the longitudinal magnetization, M_z, after inversion, and the influence of the readout blocks, based on these simulations, is shown in Figure 1. Simulations were performed for a range of T_1s (100–2000 ms) and heart rates (40–140 bpm) to test the robustness of the sequence against variations in these parameters. To determine an appropriate value for the thickness of the SS inversion pulse, a range of thicknesses (8–35 mm) were simulated for the stated range of T_1s, with a fixed image slice profile with thickness of 8 mm full width half maximum to investigate the interaction between the HS8 inversion pulse profile and the image slice profile. The inflow was not simulated, such that the performance of the sequence in measuring only the relaxation under the two different inversion conditions could be investigated to ensure that any difference measured in vivo was due to blood flow and not systematic error.

Phantom Studies

A phantom imaging study was carried out to further investigate the performance of the LL-Fair-ASL sequence in the absence of flow. The data gathered were used to investigate the dependence of T_1 and T_1^* on heart rate with the LL-FAIR-ASL sequence by plotting these values against a range of simulated heart rates. The length of the gap between the two inversion blocks (measured in heartbeats) was also varied to investigate the effect of imperfect recovery before the second inversion. These experiments were carried out on an integrated calibration phantom distributed by Dr. S. Piechnik, Oxford, for the HCMR study (Clinicaltrials.gov ID: NCT01915615). The phantom was designed to monitor stability of T_1 mapping techniques, and provides a T_1 range of ~300–3000 ms, and T_2 ~60–3000 ms. The phantom consists of nine test objects made of agar, carrageenan water gels doped with nickel chloride. The study was carried out on the 3 T scanner using a 32-channel body receive array. The simulated ECG trigger was varied from 40 bpm to 140 bpm in 20-bpm intervals. The resulting images were loaded into MATLAB for analysis, where regions of interest (ROIs) were drawn by hand within the confines of each tube and propagated throughout an image series to calculate the T_1s of the samples.

In Vivo Studies

ASL image series were acquired on 11 healthy volunteers (31 ± 7 years old; 71 ± 9 kg; two female) at 3T, in basal, mid-ventricular, and apical short axis slices using the 32-channel body receive array. All volunteers were recruited in accordance with the ethical practices of our institution and their informed consent obtained. Each of the volunteers was scanned twice, on separate days, making 22 scan sessions in total. The data from one subject was discarded due to excessive motion within the image series. In 17 of the 20 successful scans, the ASL acquisitions in the mid-ventricular slice were repeated. B_0 shimming was performed in a volume over the left

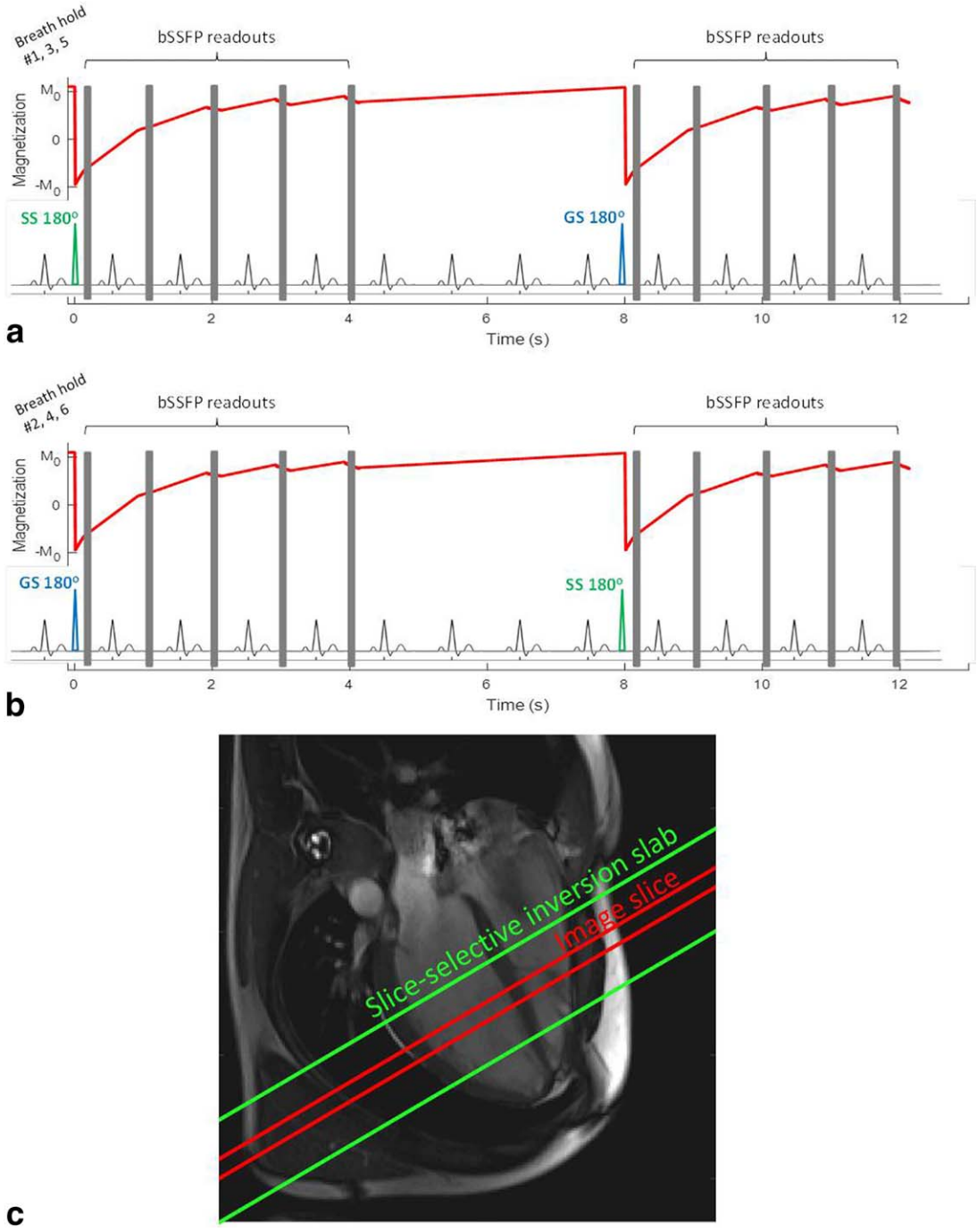

FIG. 1. A schematic of the LL-FAIR-ASL pulse sequence over 13 heartbeats for breath-holds 1, 3, and 5 (**a**) and breath-holds 2, 4, and 6 (**b**). 180° pulses (one SS, one GS, within a single breath-hold, the order of which is varied) are each followed by 5 bSSFP readouts (shown as gray boxes), separated by an R–R interval. The evolution of M_z throughout the sequence is shown in red. (**c**) A four-chamber view of the heart with the position of the imaging slice in red, and the position of the SS inversion slab in green.

ventricle (LV) covering all three slices. In each slice, the sequence as described in Figure 1 was run three times with the SS inversion block preceding the GS inversion block (called the SS-GS ordering scheme), then run a further three times with the GS inversion block preceding the SS (GS-SS), making for a total of six measurements, from which a single value of MBF could be calculated. An SS inversion thickness of 24 mm was used based on the results of the simulation and phantom scans described. This inversion slab and the imaging slice were positioned as described in Figure 1c. In all cases, ECG triggering and breath-holding were used. No motion correction or image registration was used.

Image Analysis

All image series were loaded into MATLAB and regions of interest (ROIs) were drawn by hand for both the left

ventricular myocardium and the blood pool. For the myocardium, the epicardial and endocardial borders were drawn and the myocardium divided into segments as per the American Heart Association (AHA) model (21). The apparent T_1 values (T_1^*) for the myocardium for both the SS and global inversion blocks were calculated, as was the T_1 of blood from the global data by using a three-parameter least squares fit as described by:

$$S(TI) = A - Be^{\left(-TI/T_1^*\right)} \quad [1]$$

where S was the signal intensity recorded at time TI and A, B, and T_1^* were the fitted parameters. Where T_1 values are reported, the correction described by Deichmann and Haase for FLASH images (22) and described in Eq. [2] was used, although only strictly applicable in the small tip angle regime.

$$T_1 = T_1^*\left(\frac{B}{A} - 1\right) \quad [2]$$

The phase data of the most fully recovered image from each inversion block were used to correct the polarity of the magnitude images on a pixel-by-pixel basis before fitting (23). The myocardial blood flow (MBF) for each slice was calculated from these data by the Belle quantification model (24):

$$MBF = \frac{\lambda}{T_1^{blood}}\left(\frac{T_1^{GS}}{T_1^{SS}} - 1\right) \quad [3]$$

where $\lambda = 0.92$ mL/g (25) is the blood-tissue partition coefficient of water, T_1^{blood} is the relaxation time of the blood pool and T_1^{GS} and T_1^{SS} are the values for the longitudinal relaxation time calculated for the myocardium, from the GS and SS experiment, respectively. For the in vivo study, the T_1^{GS} and T_1^{SS} values used were the observed T_1^*s. As has been discussed previously (26,27), where the Deichmann-Haase correction is used the ratio of the relaxation times remains constant $T_1{}^{\text{GS}}/T_1{}^{\text{SS}} = T_1^{*\text{GS}}/T_1^{*\text{SS}}$ as the fitted values of A and B should remain the same for both the GS and SS cases. Thus, use of the correction would have no effect on the final value of MBF. The use of T_1^* is discussed further later in this work

Reproducibility and Variability Analysis

The in vivo data were used to perform Bland-Altman analysis (28) to assess reproducibility and variation. The mean difference in each case and the value of ± 1.96 times the standard deviations (SD) were calculated, which represent the upper and lower 95% confidence bounds. When normalized to the mean value of MBF, these values give the coefficient of repeatability for both the between-session (CR_{BS}) and within-session cases (CR_{WS}). The variability of the MBF estimates was assessed by the coefficient of variation (CV, equal to the ratio of the standard deviation to the mean) for the whole sample (CV_{all}), and each subject between-session (CV_{BS}) and within-session (CV_{WS}).

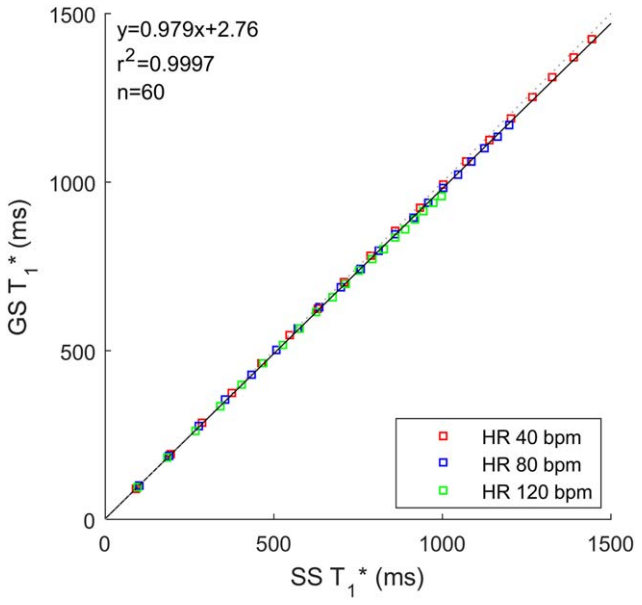

FIG. 2. Correlation plot of the simulated SS and GS T_1^* s, in the absence of flow, for heart rates of 40, 80, and 120 bpm and input T_1 values from 100 to 2000 ms (100 ms steps).

Segmental Analysis

Values of MBF were calculated for each of the 16 standard myocardial segments as defined but the AHA (21) to assess the viability of the ASL technique at segmental level. For each segment, these are reported as the mean and standard deviation across all the volunteers. The coefficient of variation (CV_{seg}) is also reported for all segments.

RESULTS

Simulation

T_1^* data were plotted for heart rates of 40, 80, and 120 bpm and for the full range of input T_1s. Figure 2 shows the simulated SS and GS T_1^*s to agree well in the absence of flow, with an R^2 value of 0.9996 and both the T_1^*s shortening with increasing heart rate.

Figure 3 shows the results of simulations to determine an appropriate value for the thickness of the SS inversion pulse. Results for both T_1 and T_1^* are plotted showing the dependence of the calculation on the extent of the inversion. The values are stable down to an inversion thickness of 23 mm then decrease with decreasing thickness. The effect is more marked with T_1 than T_1^*. For the input T_1 of 1200 ms, approximately in the myocardial range, the T_1^* drops from a maximum of 928 ms with the thickest inversion slice to 860 ms with the thinnest, a drop of 7%. The calculated T_1, however, drops from 1043 ms with the thickest slice to just 63 ms with the thinnest, a drop of 94%.

Phantom Studies

An example plot of T_1 and T_1^* against simulated heart rate is shown in Figure 4 for a gap of three heart beats. The dependence of T_1^* on heart rate can be clearly seen

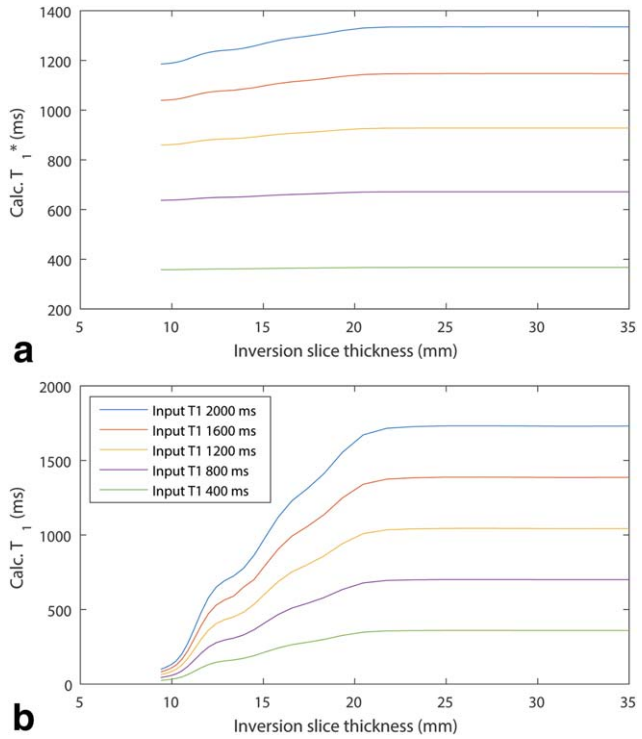

FIG. 3. For an image slice thickness of 8 mm, the SS HS8 inversion pulse width, varied from 8 to 35 mm, is plotted against the simulated observed T_1^* (**a**), and T_1 (**b**) (following the Deichmann-Haase correction) for input T_1 values of 400 to 2000 ms (400 ms steps).

for both the SS-GS and GS-SS ordering schemes, decreasing steadily as the heart rate increases. The calculated T_1, however, is stable for the first inversion block in the ordering scheme, whether SS or GS, with a value of 1431 ± 8 ms for the range of heart rates, but decreases rapidly with increasing heart rate, and, therefore, decreasing recovery time, for the second inversion block. Thus, the calculation of T_1 is dependent on the ordering scheme, whereas the calculation of the T_1^* s is not.

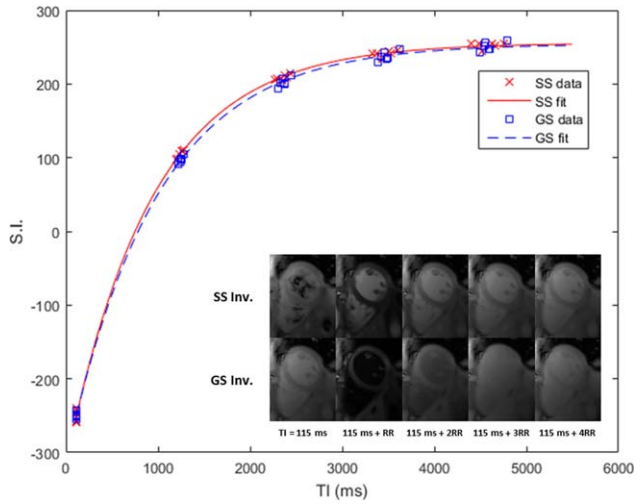

FIG. 5. A typical pair of SS and GS inversion recovery curves with data points from six breath-holds averaged over an ROI encompassing the left ventricular myocardium, and corresponding image series inset from one of the six breath-holds.

In Vivo Studies

Figure 5 shows a typical pair of T_1 recovery curves, with inset SS and GS image series. The mean MBF across all the 10 volunteers and all 2 scan sessions was 1.04 ± 0.40 mL/g/min in the basal slice, 1.06 ± 0.46 mL/g/min in the mid-ventricle and 1.06 ± 0.38 mL/g/min in the apical slice. The calculated values of MBF for each subject in each session, as well as the mean values, are presented in Figure 6. The data are presented for all scans in all three slices.

Reproducibility and Variability Analysis

Values for the coefficients of variation and reproducibility, for both the between session and within session cases, are presented in Table 1. The CV across all scans was calculated as 39, 43, and 36% in the basal, mid-

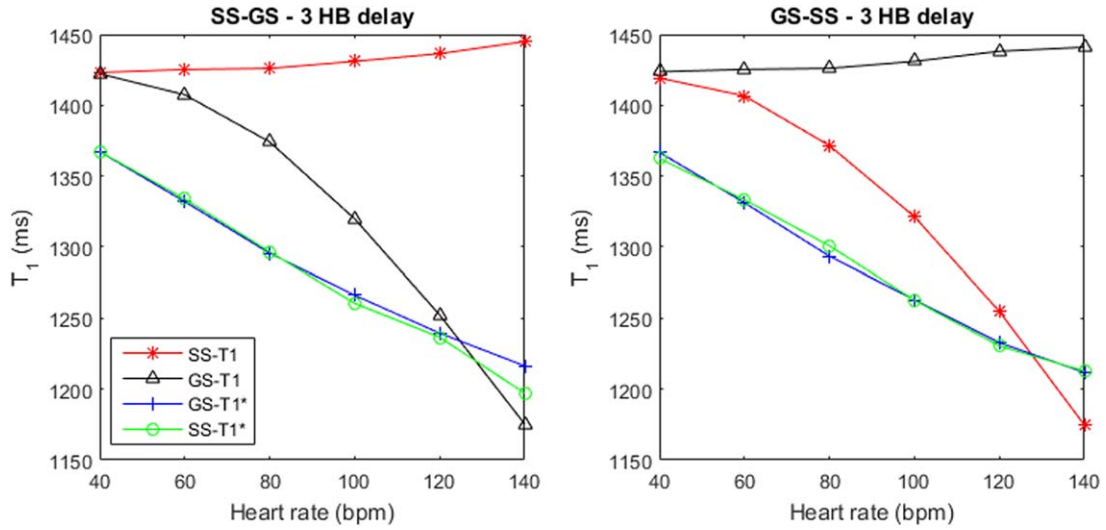

FIG. 4. Measured T_1^* and T_1 of a cardiac phantom, for both the SS and GS inversion blocks plotted against simulated heart rate, from 40–140 bpm. There was a three heartbeat delay between the end of one block and the start of the next. The data are plotted for the SS-GS (**a**) and the GS-SS (**b**) ordering scheme.

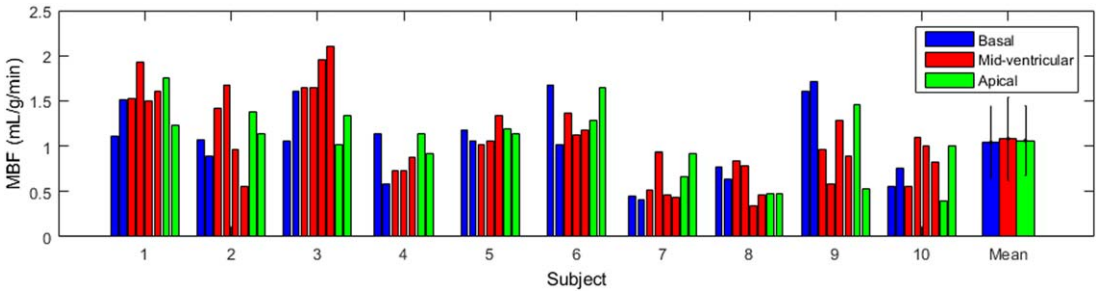

FIG. 6. Calculated MBF results for both scan sessions for all 10 volunteers in basal, mid-ventricular, and apical slices represented by blue, red, and green bars, respectively. Error bars denote the standard deviation.

ventricular, and apical slices, respectively. The CV_{BS} was 14, 16, and 17% in basal, mid, and apex; and the CV_{WS} was 13% in the mid-ventricle. The CR_{WS} was 53% in the mid-ventricle, compared with CR_{BS} values of 72, 61, and 85% in the base, mid, and apex.

Segmental Analysis

The mean values and standard deviations of segmental MBF are reported in Table 2 along with the coefficient of variation, for all 16 segments. The range of mean segmental MBF values is 0.87–1.52 mL/g/min. These values are also plotted in Figure 7a, along with previous literature values of MBF in four segments in the mid-ventricle (septum and anterior, lateral, and inferior walls) using ^{15}O PET (29). The numbering of the segments is described in Figure 7b.

DISCUSSION

In this study, a noninvasive method for quantitatively measuring myocardial blood flow using arterial spin labelling was developed and tested by means of simulation, phantom experiment and in vivo studies. The variation and reproducibility of the method were then investigated in three short axis slices, where previous cardiac ASL studies have been restricted to the mid-ventricle.

The Bloch simulations of the LL-FAIR-ASL sequence show good agreement between the SS and GS T_1^*s as presented in Figure 2. Thus, there is no dependence in the MBF calculation on error in the calculation of the T_1^* ratio. This is true of the three simulated heart rates (40, 80, and 120 bpm), despite the expected shortened T_1^* with increasing heart rate due to saturation from multiple high flip angle readouts, as seen in the simulated evolution of magnetization in Figure 1.

As observed in Figure 3, the calculation of T_1^* and T_1 is compromised at lower values of the inversion slice thickness relative to the imaging slice thickness. This occurs due to differences between the inversion profile and the image slice profile. The effect is far more marked in the calculation of T_1 due to the reliance of the Deichmann-Haase correction on inversion efficiency. At lower inversion thicknesses the efficiency is low due to the slice containing a mixture of inverted and noninverted spins. By comparison, T_1^* has little dependence on inversion efficiency, providing further motivation for its use over T_1. These data were used in the choice of inversion thickness for in vivo application of 24 mm.

Varying the simulated heart rate in the phantom scans demonstrates that the values of T_1^* are far more stable than those of T_1. Although T_1^* is dependent on heart rate, as demonstrated in Figure 4, the T_1^* values calculated for the SS and GS cases exhibit the same dependence, meaning heart rate does not bias the calculation of MBF as it is calculated from a ratio of the GS and SS T_1^*s. As discussed above, the T_1 correction is highly dependent on the inversion efficiency, and in each ASL ordering scheme the second of the two inversions suffers from apparent poor efficiency due to insufficient time for relaxation between blocks, which is necessary for achievable breath-holds. T_1^* was used for all MBF calculations as the Deichmann-Haase correction is only strictly applicable in a small angle regime and for inversion pulses applied to spins at equilibrium magnetization (22). T_1^* is independent of inversion efficiency and, as stated earlier the ratio of GS to SS T_1^*s is the same as the ratio of GS to SS T_1s.

The LL-FAIR-ASL method is attractive as it provides a noninvasive alternative to SPECT, PET, and first-pass perfusion CMR. Using this method, MBF can be measured quantitatively in a single slice in six 13-heartbeat breath-holds. Each breath-hold contains both SS and GS acquisitions, which ensures that the position of the heart and heart rate are the same for each pair. The ability to acquire an SS/GS pair in a single breath-hold is an important feature of the LL-FAIR-ASL sequence, as the measured changes in T_1^* are small and could easily be

Table 1
MBF Results from In Vivo Scans in Three Slices, Including the mean myocardial blood flow (MBF), the standard deviation and the CV across all scans and the CV and CR for between session (BS) and within session (WS) Cases

Slice	Mean MBF (mL/g/min)	SD (mL/g/min)	CV_{all} (%)	CV_{BS} (%)	CV_{WS} (%)	CR_{BS} (%)	CR_{WS} (%)
Basal	1.04	0.40	39	14		72	
Mid	1.06	0.46	43	16	13	61	53
Apical	1.06	0.38	36	17		85	

Table 2
Mean MBF Values for Each Segment, Where Segments 1-6 Are the Basal Slice, 7-12 Are the Mid-ventricular Slice, and 13-16 Are the Apical Slice

Segment	Mean MBF (mL/g/min)	SD (mL/g/min)	CV_{seg} (%)
1	0.97	0.6	62
2	1.22	0.91	75
3	1.14	0.88	77
4	0.88	0.74	84
5	1.12	0.59	53
6	1.33	0.65	49
7	1.09	0.73	67
8	1.15	0.66	57
9	1.06	1.04	98
10	0.87	0.51	59
11	1.18	0.61	52
12	1.38	0.83	60
13	0.97	0.89	92
14	0.98	0.67	68
15	1.52	0.95	63
16	1.19	0.76	64

lost among systematic errors. The mean MBF, in the mid-ventricular slice, of 1.06 ± 0.46 mL/g/min compares well with literature values, as presented in Table 3 (29–36).

While reproducibility and variability of similar techniques have been investigated in mice (37,38), to our knowledge this has not been carried out in human myocardium. Resting MBF values for healthy volunteers have previously been shown to be heterogeneous in studies using PET (29) and first-pass perfusion CMR (39). The high observed values for CV_{all} across all subjects, 39, 43, and 36% for basal, mid, and apical slices, respectively, show that our results reflect this heterogeneous nature. This variability, calculated as the coefficient of variation is comparable to similar measures reported for preclinical cardiac ASL (37,38).

The values of CV_{BS} and CV_{WS} calculated for individual subjects were all below the values reported for CV_{all} except for a single apical slice which gave a CV_{BS} of 43%. However, the mean values of CV_{BS} for each slice and CV_{WS} for the mid slice only, are significantly lower than CV_{all}, with a maximum of 17%. This shows that the variation in results exhibited by an individual subject in each case is much less than across the population as a whole. The CV_{BS} shows the variation due to the method, plus re-setup effects such as repositioning, re-localization, re-shimming etc. The CV_{WS} primarily reflects the methodological effects.

The Bland-Altman analysis showed the mean difference in both the between-session case for all three slices and the within-session case, for the mid slice only, to be close to zero and all bar one of the data points to lie within the ± 1.96 SD bounds. The values of CR give an indication of the change in MBF required to be detected above systematic errors. The between-session CRs of 72, 61, and 85% for the basal, mid, and apical slices, show the level of repeatability expected across repeat scans. They show the change in MBF required to show a difference over time and is useful to consider if planning a longitudinal study in a patient group. The within-session CR of 53% for the mid-ventricular slice gives a useful indication of the detectable change in MBF. Thus, a change in MBF would be reliably detectable when rising from the mean mid-ventricular MBF, measured with LL-FAIR-ASL, of 1.08 mL/g/min to a value of 1.74 mL/g/min between-session and 1.65 mL/g/min within-session. During vasodilator stress, the change in MBF in non-ischemic segments of the heart has been shown to be between 300 and 420% (35,40,41), or between 3.24 and 4.54 mL/g/min based on the mean mid-ventricular MBF reported here. Therefore, the expected change in global MBF under stress should be detectable with the LL-FAIR-ASL method.

Segmental MBF is an important measure in disease, as it allows investigation of MBF changes in the arterial territories of the myocardium. Previous publications using PET (29) and ASL (35) have commented on the spatial heterogeneity of resting MBF within a slice. The relative dispersion, here called the coefficient of variation, was

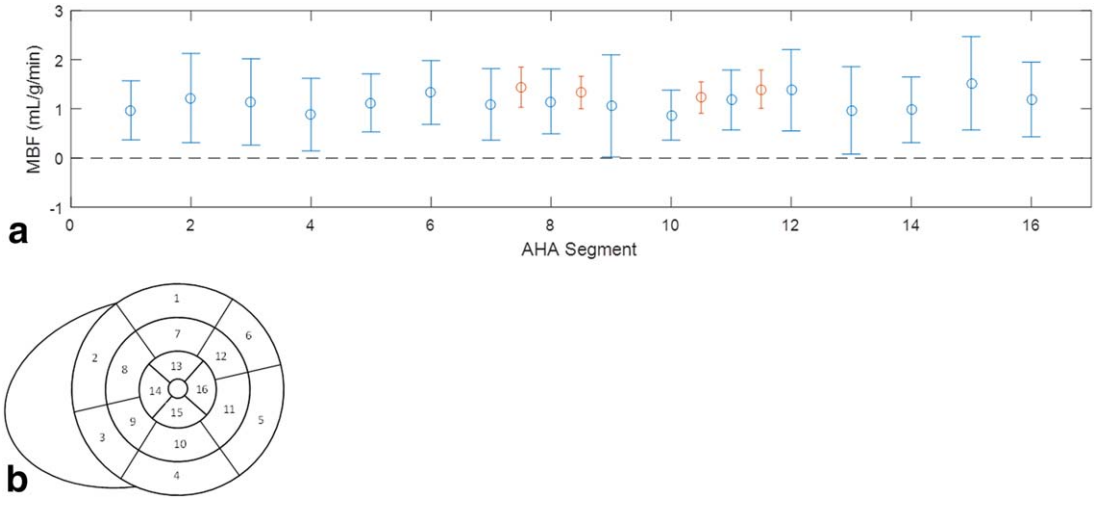

FIG. 7. The mean ± standard deviation of MBF across all subjects for each myocardial segment as defined by the AHA (**a**), as described in (**b**), where segments 1–6 are the basal slice, 7–12 are the mid-ventricular slice, and 13–16 are the apical slice. The data points in red are literature values in the septum and anterior, lateral and inferior walls of the mid–ventricle from Chareonthaitawee et al 2001 (29).

Table 3
Comparison of LL-FAIR Mid-ventricular Resting MBF against Literature Values for Previous Cardiac ASL Methods, First-Pass Perfusion CMR, and PET

Source	Method	Age (y)	Gender	Population	MBF_{rest} (mL/g/min)
LL-FAIR-ASL	ASL	31 ± 7	8 M/2 F	Healthy	1.06 ± 0.46
Zun 2009(36)	ASL		8 M/2 F	Healthy	1.36 ± 0.40
Zun 2011(35)	ASL	64 ± 11	10 M/19 F	CAD patients	0.97 ± 0.64
Wang 2010(34)	ASL	39 ± 9	10 M/1 F	Healthy	1.00 ± 0.55
Northrup 2008(33)	ASL	22 ± 2	5 M/3 F	Healthy	1.06 ± 0.19
Jerosch-Herold 2008(31)	CMR - First Pass	63 ± 10	11 M/19 F	Atherosclerosis	1.01 ± 0.22/ 0.91 ± 0.18[a]
Hsu 2006(30)	CMR - First Pass	33 ± 4	2 M/8 F	Healthy	1.02 ± 0.22
Manabe 2009(32)	^{82}Rb PET	29 ± 9	8 M/7 F	Healthy	0.99 ± 0.29/ 1.00 ± 0.25*
Chareonthaitawee 2001(29)	^{15}O PET	46 ± 12	131 M/38 F	Healthy	1.33 ± 0.32

[a]Results from two separate exams on the same group of patients/volunteers.

reported as 13% with PET and 68% (range, 11% to 152%) with ASL, compared with 67% (with a range of 49% to 98%) with LL-FAIR-ASL. This difference in error between the ASL methods and PET is also reflected in the data plotted in Figure 7 and is perhaps expected given the inherently low signal-to-noise ratio of the method and the low resolution of the PET method, noted as a limitation by the authors and reported as $8.43 \times 8.33 \times 6.6\,mm^3$ full-width half maximum compared with $1.7 \times 2.2 \times 8\,mm^3$ with LL-FAIR-ASL. However, given the expected increase in MBF under stress, the difference in perfusion reserve between ischemic and normal segments, should be detectable.

This study served to validate the LL-FAIR-ASL technique for measurement of resting MBF in healthy humans. Future studies will be required to validate the method in patient populations under stress and compare the results with standard methods such as first-pass perfusion CMR. Image registration methods may be used to compensate for residual motion within breath-holds, particularly in studies involving patients. In addition, more complex models for quantification of MBF, taking account of such effects as arterial transit time, the partial inversion of the blood pool during SS inversion and the perturbation of the inversion recovery by the readouts could be implemented. However, these studies are beyond the scope of this work.

CONCLUSIONS

The LL-FAIR-ASL sequence for quantitative measurement of MBF was shown to be robust and efficient when performed in vivo. The method is completely noninvasive, not requiring contrast agent, and provides resting MBF values in healthy volunteers which compare well with the literature and display the previously reported heterogeneity within healthy volunteer groups. MBF values are reported globally in three slices with a cardiac ASL technique for the first time. The variability of the method was shown to compare favorably with published values in similar techniques used in preclinical imaging but, to our knowledge, has not previously been performed in human volunteers. The method was shown to be sensitive enough to detect MBF increase under stress conditions in future studies. The presented results should prove useful in the planning of clinical research studies using this sequence to quantitatively measure MBF at rest and under stress in healthy volunteers or in patient groups.

ACKNOWLEDGMENT

C.T.R. is funded by the Wellcome Trust and the Royal Society.

REFERENCES

1. Pennell DJ, Sechtem UP, Higgins CB, Manning WJ, Pohost GM, Rademakers FE, van Rossum AC, Shaw LJ, Yucel EK. Clinical indications for cardiovascular magnetic resonance (CMR): Consensus Panel report. Eur Heart J 2004;25:1940–1965.
2. Gerber BL, Raman SV, Nayak K, Epstein FH, Ferreira P, Axel L, Kraitchman DL. Myocardial first-pass perfusion cardiovascular magnetic resonance: history, theory, and current state of the art. J Cardiovasc Magn Reson 2008;10:18.
3. Di Bella EV, Parker DL, Sinusas AJ. On the dark rim artifact in dynamic contrast-enhanced MRI myocardial perfusion studies. Magn Reson Med 2005;54:1295–1299.
4. Sieber MA, Lengsfeld P, Walter J, Schirmer H, Frenzel T, Siegmund F, Weinmann HJ, Pietsch H. Gadolinium-based contrast agents and their potential role in the pathogenesis of nephrogenic systemic fibrosis: the role of excess ligand. J Magn Reson Imaging 2008;27:955–962.
5. Ben-Haim S, Murthy VL, Breault C, et al. Quantification of myocardial perfusion reserve using dynamic SPECT imaging in humans: a feasibility study. J Nucl Med 2013;54:873–879.
6. Garcia EV. Are SPECT measurements of myocardial blood flow and flow reserve ready for clinical use? Eur J Nucl Med Mol Imaging 2014;41:2291–2293.
7. Bergmann SR, Herrero P, Markham J, Weinheimer CJ, Walsh MN. Noninvasive quantitation of myocardial blood-flow in human-subjects with oxygen-15-labeled water and positron emission tomography. J Am Coll Cardiol 1989;14:639–652.
8. Lortie M, Beanlands RSB, Yoshinaga K, Klein R, DaSilva JN, Dekemp RA. Quantification of myocardial blood flow with Rb-82 dynamic PET imaging. Eur J Nucl Med Mol Imaging 2007;34:1765–1774.
9. Detre JA, Leigh JS, Williams DS, Koretsky AP. Perfusion imaging. Magn Reson Med 1992;23:37–45.
10. Detre JA, Zhang W, Roberts DA, Silva AC, Williams DS, Grandis DJ, Koretsky AP, Leigh JS. Tissue specific perfusion imaging using arterial spin labeling. NMR in biomedicine 1994;7:75–82.
11. Kim SG. Quantification of relative cerebral blood flow change by flow-sensitive alternating inversion recovery (FAIR) technique: application to functional mapping. Magn Reson Med 1995;34:293–301.
12. Kim SG, Tsekos NV. Perfusion imaging by a flow-sensitive alternating inversion recovery (FAIR) technique: application to functional brain imaging. Magn Reson Med 1997;37:425–435.
13. Moon JC, Messroghli DR, Kellman P, et al. Myocardial T1 mapping and extracellular volume quantification: a Society for Cardiovascular

Magnetic Resonance (SCMR) and CMR Working Group of the European Society of Cardiology consensus statement. J Cardiovasc Magn Reson 2013;15:92.
14. Piechnik SK, Ferreira VM, Dall'Armellina E, Cochlin LE, Greiser A, Neubauer S, Robson MD. Shortened Modified Look-Locker Inversion recovery (ShMOLLI) for clinical myocardial T1-mapping at 1.5 and 3 T within a 9 heartbeat breathhold. J Cardiovasc Magn Reson 2010; 12:69.
15. Messroghli DR, Radjenovic A, Kozerke S, Higgins DM, Sivananthan MU, Ridgway JP. Modified Look-Locker inversion recovery (MOLLI) for high-resolution T1 mapping of the heart. Magn Reson Med 2004; 52:141–146.
16. Look DC, Locker DR. Time saving in measurement of NMR and EPR relaxation times. Rev Sci Instrum 1970;41:250.
17. Keith GA RC, Chappell, MA, Robson MD. A Look-Locker acquisition scheme for quantitative myocardial perfusion imaging by arterial spin labelling in humans at 3 T. In Proceedings of the 23rd Annual Meeting of ISMRM, Toronto, 2015. Abstract 2690.
18. Tannus A, Garwood M. Adiabatic pulses. NMR in biomedicine 1997; 10:423–434.
19. Schar M, Kozerke S, Fischer SE, Boesiger P. Cardiac SSFP imaging at 3 Tesla. Magn Reson Med 2004;51:799–806.
20. Do HP, Jao TR, Nayak KS. Myocardial arterial spin labeling perfusion imaging with improved sensitivity. J Cardiovasc Magn Reson 2014; 16:15.
21. Cerqueira MD, Weissman NJ, Dilsizian V, et al. Standardized myocardial segmentation and nomenclature for tomographic imaging of the heart - a statement for healthcare professionals from the Cardiac Imaging Committee of the Council on Clinical Cardiology of the American Heart Association. Circulation 2002;105:539–542.
22. Deichmann R, Haase A. Quantification of T1 values by Snapshot-Flash NMR Imaging. J Magn Reson 1992;96:608–612.
23. Gowland PA, Leach MO. A simple method for the restoration of signal polarity in multi-image inversion recovery sequences for measuring T1. Magn Reson Med 1991;18:224–231.
24. Belle V, Kahler E, Waller C, Rommel E, Voll S, Hiller KH, Bauer WR, Haase A. In vivo quantitative mapping of cardiac perfusion in rats using a noninvasive MR spin-labeling method. J Magn Reson Imaging 1998;8:1240–1245.
25. Bergmann SR, Fox KA, Rand AL, McElvany KD, Welch MJ, Markham J, Sobel BE. Quantification of regional myocardial blood flow in vivo with H215O. Circulation 1984;70:724–733.
26. Kampf T, Helluy X, Gutjahr FT, Winter P, Meyer CB, Jakob PM, Bauer WR, Ziener CH. Myocardial perfusion quantification using the T1-based FAIR-ASL method: the influence of heart anatomy, cardiopulmonary blood flow and look-locker readout. Magn Reson Med 2014;71:1784–1797.
27. Streif JUG, Hiller KH, Waller C, Nahrendorf M, Wiesmann F, Bauer WR, Rommel E, Haase A. In vivo assessment of absolute perfusion in the murine skeletal muscle with spin labeling MRI. J Magn Reson Imaging 2003;17:147–152.
28. Bland JM, Altman DG. Statistical methods for assessing agreement between two methods of clinical measurement. Lancet 1986;1:307–310.
29. Chareonthaitawee P, Kaufmann PA, Rimoldi O, Camici PG. Heterogeneity of resting and hyperemic myocardial blood flow in healthy humans. Cardiovasc Res 2001;50:151–161.
30. Hsu LY, Rhoads KL, Holly JE, Kellman P, Aletras AH, Arai AE. Quantitative myocardial perfusion analysis with a dual-bolus contrast-enhanced first-pass MRI technique in humans. J Magn Reson Imaging 2006;23:315–322.
31. Jerosch-Herold M, Vazquez G, Wang L, Jacobs DR Jr, Folsom AR. Variability of myocardial blood flow measurements by magnetic resonance imaging in the multi-ethnic study of atherosclerosis. Invest Radiol 2008;43:155–161.
32. Manabe O, Yoshinaga K, Katoh C, Naya M, deKemp RA, Tamaki N. Repeatability of rest and hyperemic myocardial blood flow measurements with 82Rb dynamic PET. J Nucl Med 2009;50:68–71.
33. Northrup BE, McCommis KS, Zhang H, Ray S, Woodard PK, Gropler RJ, Zheng J. Resting myocardial perfusion quantification with CMR arterial spin labeling at 1.5 T and 3.0 T. J Cardiovasc Magn Reson 2008;10:53.
34. Wang DJ, Bi X, Avants BB, Meng T, Zuehlsdorff S, Detre JA. Estimation of perfusion and arterial transit time in myocardium using free-breathing myocardial arterial spin labeling with navigator-echo. Magn Reson Med 2010;64:1289–1295.
35. Zun Z, Varadarajan P, Pai RG, Wong EC, Nayak KS. Arterial spin labeled CMR detects clinically relevant increase in myocardial blood flow with vasodilation. JACC Cardiovasc Imaging 2011;4:1253–1261.
36. Zun Z, Wong EC, Nayak KS. Assessment of myocardial blood flow (MBF) in humans using arterial spin labeling (ASL): feasibility and noise analysis. Magn Reson Med 2009;62:975–983.
37. Campbell-Washburn AE, Price AN, Wells JA, Thomas DL, Ordidge RJ, Lythgoe MF. Cardiac arterial spin labeling using segmented ECG-gated Look-Locker FAIR: variability and repeatability in preclinical studies. Magn Reson Med 2013;69:238–247.
38. Naresh NK, Chen X, Moran E, Tian Y, French BA, Epstein FH. Repeatability and variability of myocardial perfusion imaging techniques in mice: comparison of arterial spin labeling and first-pass contrast-enhanced MRI. Magn Reson Med 2016;75:2394–2405.
39. Greve AM HL, Vasu S, Bendettini, WP, Arai AE. Heterogeneity of resting and hyperemic myocardial blood flow in healthy volunteers: a quantitative CMR perfusion pixel-map study. J Cardiovasc Magn Reson 2014;16(Suppl 1):21.
40. Abdelmoneim SS, Dhoble A, Bernier M, Moir S, Hagen ME, Ness SAC, Abdel-Kader SS, Pellikka PA, Mulvagh SL. Absolute myocardial blood flow determination using real-time myocardial contrast echocardiography during adenosine stress: comparison with single-photon emission computed tomography. Heart 2009;95:1662–1668.
41. Wyss CA, Koepfli P, Mikolajczyk K, Burger C, von Schulthess GK, Kaufmann PA. Bicycle exercise stress in PET for assessment of coronary flow reserve: repeatability and comparison with adenosine stress. J Nucl Med 2003;44:146–154.